ISBN: 978-3-95450-227-1 ISSN: 2673-5490 doi:10.18429/JACoW-IPAC2022-TUPOPT068

TRANSVERSE AND LONGITUDINAL MODULATION OF PHOTOINJECTION PULSES AT FLUTE

M. Nabinger*†, C. Sax*, M. J. Nasse, J. Schäfer, C. Widmann, C. Xu, A.-S. Müller
Karlsruhe Institute of Technology, Karlsruhe, Germany

Abstract

To generate the electrons to be accelerated, a photoinjection laser is used at the linac-based test facility FLUTE (Ferninfrarot Linac- Und Test Experiment) at the Karlsruhe Institute of Technology (KIT). The properties of the laser pulse, such as intensity, laser spot size or temporal profile, are the first parameters to influence the characteristics of the electron bunches. In order to control the initial parameters of the electrons in the most flexible way possible, the laser optics at FLUTE are therefore supplemented by additional setups that allow transverse and longitudinal laser pulse shaping by using spatial light modulators (SLMs). In the future, the control of the SLMs will be integrated into a machine learning (ML) supported feedback system for the optimization of the electron bunch properties. In this contribution, the first test experiments and results on laser pulse shaping at FLUTE on the way to this project are presented.

INTRODUCTION

Modern and future accelerator projects require electron beams with an exceptional combination of high brightness and low emittance. As a consequence, in recent years there has been a strong interest in the improvement of RF photoinjectors [1–3]. Of particular interest is the tailoring of the photoinjection pulse properties [4]. Arbitrary shaping of the drive laser pulse in both transverse and longitudinal directions provides a powerful tool to significantly influence and control the electron bunch characteristics.

Among the most promising devices for realizing individual pulse shaping are liquid crystal SLMs, pixel-based electro-optical components that allow a modulation in phase and/or intensity of the incident light. The working principle of the phase-only modulating SLMs, which are used in this work, is shown in Fig. 1. The birefringent liquid crystal molecules (LCM) are embedded in several cells/pixels between pairs of electrodes on a silicon substrate, protected by a glass layer on top. In such a setup - also known as liquid crystals on silicon (LCoS) - the orientation of the LCM can be changed by applying a voltage to the cell, which leads to a change of the effective refractive index seen by the incident light wave. As a result, the phase of the reflected wave can be modulated for every pixel independently.

In order to create arbitrary images, the voltages corresponding to the phase shift for each single pixel in the array must be controlled entirely. This is achievable by computing and applying a 2D phase distribution or *phase mask*, also known as a computer generated hologram (CGH). For the calculation of a CGH, several algorithms can be used, for instance the Gerchberg-Saxton (GS) algorithm, which is based on inverse Fourier transforms.

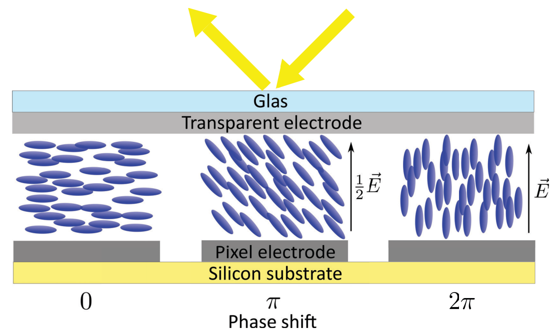

Figure 1: Working principle of an SLM with embedded LCM. By applying a voltage, the orientation of the LCM can be changed and thus the phase of the incident light can be modulated.

At the linac-based test facility FLUTE at KIT, a 800 nm Ti:Sa laser with 35 fs bandwith-limited pulse length is used for photoinjection. The copper photocathode requires a conversion of the wavelength to 266 nm by third harmonic generation. Such nonlinear processes and also the subsequent relatively complex beam path with many optical elements are difficult to take into account in the conventional calculation of CGHs. This leads to distortions of the final image on the photocathode. Hence, a simple application of the GS algorithm is insufficient. Therefore, first approaches to ML-assisted control of pulse modulation by SLMs have been introduced [5, 6]. Recently, promising attempts have been investigated and further developed at FLUTE [7].

In this paper, we present two test setups and the achieved results for transverse and longitudinal pulse shaping using a LCoS-SLM at FLUTE at KIT. Here, a commercially available Hamamatsu LCoS-SLM X13138-02 optimized for a wavelength range of 800 nm ± 50 nm with a resolution of 1024×1272 pixels was used. In addition, a first integration of an SLM into the photoinjection path of FLUTE was realized. We present the first transversely modulated photoinjection pulses at FLUTE and the resulting double electron beam.

PULSE SHAPING TEST SETUPS

Transverse Modulation

As schematically shown in Fig. 2a, the transversal test setup was realized by using a widened linearly polarized red alignment laser of 638 nm wavelength to allow simple initial optimization of the CGH calculations. Despite the wavelength mismatch in terms of optimal use, the SLM

* Both authors have contributed equally.
† matthias.nabinger@kit.edu

ISBN: 978-3-95450-227-1 ISSN: 2673-5490 doi:10.18429/JACoW-IPAC2022-TUPOPT068

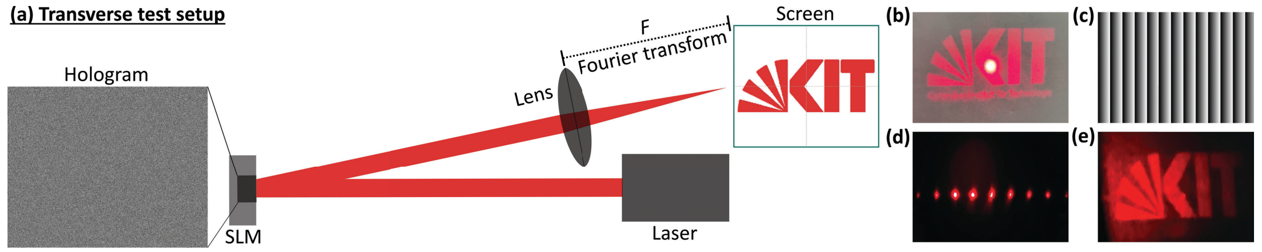

Figure 2: (a) Schematic drawing of the transverse pulse modulation test setup at FLUTE. The laser light (here 638 nm) is modulated by the SLM using a calculated hologram. Afterwards it is displayed as an amplitude image via a Fourier transform in the focal plane of a converging lens. (b) Amplitude image of the 'KIT' logo with clearly visible zero-order beam (unmodulated light). (c) Blazed grating phase mask and (d) resulting splitting into the different diffraction orders. (e) Amplitude image of the 'KIT' logo with suppressed zero-order beam by superpositioning the phase mask from (c) and only using the first diffraction order of (d).

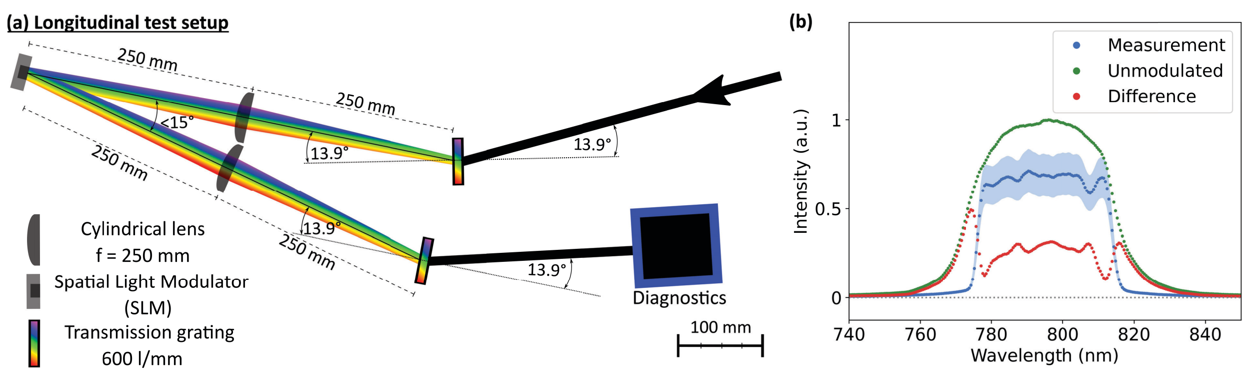

Figure 3: (a) Schematic drawing of the longitudinal pulse modulation test setup at FLUTE. The incident laser pulse is first split into its spectral components via a transmission grating and then imaged by a cylindrical lens onto the SLM. After modulating the imaged line spectrum, the pulse is spectrally reassembled and measured. (b) Measurement result (blue with uncertainty band) of generated spectral top-hat pulse shape. The unmodulated pulse is shown in green, the difference in red.

still functions acceptably in the visible red spectrum. After coupling the laser light onto the SLM surface, a CGH was calculated with an in-house developed Python program using the GS algorithm and applied to the device. Subsequently, the reflected beam was sent through a lens, here acting as a Fourier lens, resulting in an amplitude image in the focal plane. By this, arbitrary manipulations in the image plane can be achieved, for example a picture of the 'KIT'-logo (Fig. 2b).

In order to eliminate the strong unmodulated light component (also called *zero-order beam)* visible in the middle of the amplitude image generated in this way, different approaches [8] were tested. One possibility is to use a blazed-grating phase mask (Fig. 2c) and consequently split the light into different diffraction orders (Fig. 2d). Applying the superposition-principle, i.e. adding up the CGH from Fig. 2a and the grating from Fig. 2c would result in multiple copies of the image, one for each diffraction order. Since only the zeroth diffraction order contains unmodulated components, these can be successfully suppressed by filtering a higher order (Fig. 2e).

Longitudinal Modulation

A longitudinal modulation of the laser pulse shape with a phase-only SLM can be achieved via a modulation of the different spectral components of the laser pulse. To do this, the spectral components are imaged on the pixels of the SLM. For the longitudinal tests at FLUTE we used the setup illustrated in Fig. 3a. The ultra-short laser pulse is spatially split in its spectral components with a transmission grating. The spectrum is imaged via a cylindrical lens onto the SLM surface and can then be modulated individually.

The subsequent reassembling of the pulse is realized by a mirrored imaging system, so that all optical components form a well known zero-dispersion-4f-system [9]. Afterwards, diagnostics like an autocorrelator can be used to measure and characterize the temporal properties of the modulated pulse or a spectrometer to analyze the spectral shape. For the ideal arrangement of all components shown in Fig. 3a simulations were performed in advance to achieve the best possible resolution for the available SLM size (not shown here, see [10]).

We used this setup to generate a *spectral* top-hat pulse, as shown in Fig. 3b. The measured unmodulated reference laser pulse from the FLUTE photoinjection Ti:Sa laser system (green curve) with a spectral range from 760 nm to

ISBN: 978-3-95450-227-1 ISSN: 2673-5490 doi:10.18429/JACoW-IPAC2022-TUPOPT068

830 nm was modulated using a blazed grating phase mask with horizontal blaze lines, leading to a diffraction in vertical direction. Vertical stripes with the horizontal grating lines on the SLM allow the control of each wavelength individually. By looking at a side order, one can not only avoid interfering unmodulated (zero-order beam) parts, but also regulate the intensity of the spectral components by choosing the appropriate blaze angle. Thus, the frequency range of interest can be attenuated and for example fringe regions of the spectrum can be eliminated. The next step planned is to move from a spectral top-hat pulse shape to a temporal one. To do this, the spectrum must be modulated with a sinc function, which corresponds to the Fourier transform of the top-hat function from time to the frequency domain.

PHOTOINJECTION PULSE MODULATION

Recently, initial experiments on modulation of photoinjection pulses have been performed at FLUTE. For this purpose, an LCoS-SLM was integrated into the beam path using a pair of flip mirrors to allow easy switching between beam operation with and without SLM. In this setup, the SLM was placed in the beam path to the electron gun approximately 40 m before the photocathode surface.

For the first photoinjection pulse modulation experiments, a blazed grating phase mask was used again. Here the programmed grating properties, like grating constant and blaze angle, were chosen in such a way that the zeroth and first diffraction order could both be observed on the cathode surface with a similar intensity and a separation in the sub-millimeter range. After modulation, the effects on the resulting electron beam were observed.

The results of the experiment are shown in Fig. 4 as false-color images of the laser intensity on the cathode surface (left column) and the electron density on a YAG screen (right column), respectively. The screen for electron detection is placed at the end of the beamline at about 3 m after the cathode. As expected, a division of the laser spot into 2 focal points could be observed on the cathode. As a guide to the eye, a dashed white line was drawn through the reference spot to show the left-shifted modulated first diffraction order. Since the overall intensity was not changed, the weaker pulses can be explained by the intensity splitting as well as modulation losses.

As a direct consequence of the two laser pulses on the cathode, the generation of two co-propagating electron beams was observed (Fig. 4 bottom right). Similar to the laser intensity, less charge per electron bunch could be detected and the first order beam was a bit weaker than the zeroth order beam. Also noticeable is the vertical offset of the second bunch, which is due to the off-axis propagation relative to the solenoid's magnetic axis. This effect is to be expected if the beam axis does not coincide with the magnetic axis [11], and could be used to perform specific and efficient studies on the alignment of a solenoid magnet in comparable machines.

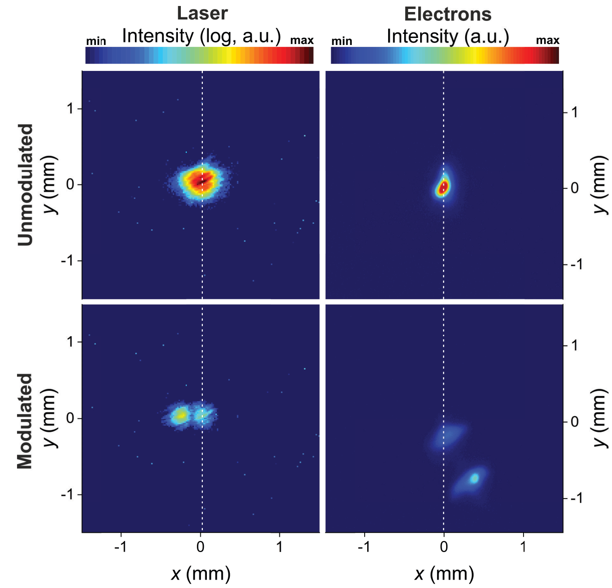

Figure 4: False color images of the photoinjection UV laser pulse on the cathode seen by a camera (left column) and the resulting electron beam visualized on a YAG screen (right column). In the top row, the unmodulated laser and electron spot is shown. In the bottom row, the laser pulse was transversely modulated via a blazed-grating phase mask on the SLM causing the emergence of a second laser spot (first diffraction order), which in the end is resulting in a double co-propagating electron beam. Corresponding reference laser pulses or electron bunches (zeroth diffraction order) were marked with a white dashed line as a guide to the eye.

SUMMARY AND OUTLOOK

At the linac-based test facility FLUTE at KIT, two laser shaping setups were realized for transverse and longitudinal pulse modulation. Here, a calculation of CGHs for the generation of arbitrary amplitude images was implemented. In addition, measures for the reduction of unmodulated light components were tested and a spectral top-hat pulse shape could be successfully generated. Furthermore, a first implementation of an SLM in the photoinjection path at FLUTE was realized, resulting in the creation of spatially displaced co-propagating electron bunches. This represents a crucial step for future advanced beam modulation projects to study bunch and machine characteristics, and also paves the way towards an ML-supported feedback system including injection laser and machine parameters.

ACKNOWLEDGEMENTS

We thank E. Bründermann for valuable ideas and comments. M. N., J. S. and C. X. acknowledge support by the Doctoral School "Karlsruhe School of Elementary and Astroparticle Physics: Science and Technology" (KSETA).

REFERENCES

[1] R. Akre *et al.*, "Commissioning the Linac Coherent Light Source injector", *Phys. Rev. ST Accel. Beams*, vol. 11,

p. 030703, Mar. 2008. doi:10.1103/PhysRevSTAB.11.030703

[2] F. Stephan *et al.*, "Detailed characterization of electron sources yielding first demonstration of European X-ray Free-Electron Laser beam quality", *Phys. Rev. ST Accel. Beams*, vol. 13, p. 020704, Feb. 2010. doi:10.1103/PhysRevSTAB.13.020704

[3] C.M. Pierce *et al.*, "Low intrinsic emittance in modern photoinjector brightness", *Phys. Rev. Accel. Beams*, vol. 23, p. 070101, Jul. 2020. doi:10.1103/PhysRevAccelBeams.23.070101

[4] Y. Li, S. Chemerisov, and J. Lewellen, "Laser pulse shaping for generating uniform three-dimensional ellipsoidal electron beams", *Phys. Rev. ST Accel. Beams*, vol. 12, p. 020702, Feb. 2009. doi:10.1103/PhysRevSTAB.12.020702

[5] A. Sinha, J. Lee, S. Li, and G. Barbastathis, "Lensless computational imaging through deep learning", *Optica*, vol. 4, pp. 1117–1125, 2017. doi:10.1364/OPTICA.4.001117

[6] R. Horisaki, R. Takagi, and J. Tanida, "Deep-learning-generated holography", *Appl. Opt.*, vol. 57, pp. 3859–3863, 2018. doi:10.1364/AO.57.003859

[7] C. Xu *et al.*, “Machine Learning Based Spatial Light Modulator Control for the Photoinjector Laser at FLUTE”, in *Proc. IPAC'21*, Campinas, Brazil, May 2021, pp. 3332–3335. doi:10.18429/JACoW-IPAC2021-WEPAB289

[8] H. Zhang, J. Xie, J. Liu, and Y. Wang, "Elimination of a zero-order beam induced by a pixelated spatial light modulator for holographic projection", *Appl. Opt.*, vol. 48, pp. 5834–5841, 2009. doi:10.1364/AO.48.005834

[9] F.Z. Duan, X.H. Yang, Y.M. Nie, and J.L. Qi, "A Nested Folded 4f System for Ultra-Short Optical Pulse Shaping by Liquid Crystal Spatial Light Modulator", *Applied Mechanics and Materials*, vol. 556–562, pp. 1704–1707, 2014. doi:10.4028/www.scientific.net/AMM.556-562.1704

[10] C. Sax, "Aufbau und Test eines flexiblen Laserpuls-Strahlformungssystems für den FLUTE Photoinjektor zur Kontrolle von Elektronenpaketen", Master thesis, Phys. Dept., Karlsruher Institut für Technologie, Karlsruhe, Germany, 2021. doi:10.5445/IR/1000146789

[11] S. Yamin, R.W. Assmann, and B. Marchetti, "Study for the alignment of focusing solenoid of ares rf gun and effect of misalignment of solenoid on emittance of space charge dominated electron beam", *J. Phys.: Conf. Ser.*, vol. 1350, p. 012014, Nov. 2019. doi:10.1088/1742-6596/1350/1/012014